Building Tomorrow's Society

Bâtir la Société de Demain

Fredericton, Canada

June 13 – June 16, 2018/ *Juin 13 – Juin 16, 2018*

FINITE ELEMENT ANALYSIS OF IN-SITU DECOMMISSIONED STEEL PIPELINES SUBJECTED TO SURFACE LIVE LOAD

Walsh, Coltin[1] and El-Badry, Mamdouh[1,2]
[1] University of Calgary, Canada
[2] melbadry@ucalgary.ca

Abstract: Steel pipelines are used throughout the energy industry as the primary means of transporting natural gas, crude oil and petroleum-related products and chemicals. When a pipeline permanently ceases operation, it is decommissioned and may be left in place underground. Over time, the pipeline will degrade due to environmental and in-*situ* conditions. Corrosion is the principal mechanism for the degradation of decommissioned pipelines. Corrosion and degradation reduce the material strength and stiffness of the pipe. Degraded pipes may no longer be capable of bearing the loads imposed by groundcover and surface vehicles. Potential collapse of decommissioned pipelines poses a risk to both the public and the environment. The static structural response of buried decommissioned pipelines subjected to surface load is analyzed using the finite element software ABAQUS. The buried pipeline is modelled within a uniform soil block, eliminating the effects of boundary conditions. Soil-pipe interaction is considered assuming a frictional slippage contact definition. The pipe is subjected to both overburden dead load and surface live load. Surface live load is taken as the maximum axle load of a CL-800 truck using an appropriate dynamic loading factor. The effects of various in-*situ* parameters including the depth of bury, pipe diameter and wall thickness are investigated. The results indicate that for reasonable depths of bury, soil stiffness, pipe diameter and wall thickness, the maximum stresses lie below the elastic limit. However, for shallow depths of bury, local deformations and stresses become significant and increase rapidly.

Keywords: buried pipeline; corrosion; finite element analysis; soil-pipe interaction; stress

1 INTRODUCTION

Steel pipelines are being used by the energy-related industry in North America as the primary means of transporting crude oil, natural gas and petro-chemical products. In Canada alone, the energy pipelines extend along more than 700,000 km (Nazemi and Das 2010). The majority of these pipelines run underground. At the end of a pipeline's useful life, it is decommissioned and may be removed or left in place underground. When a decommissioned pipeline is left underground, various corrosion protection methods are terminated, no longer maintained, or degrade over time. As a result, the pipeline begins to corrode. Corrosion is the primary cause of structural degradation of decommissioned pipelines. Such degradation results in a reduction of the bearing capacity and the pipeline may no longer be capable of bearing the imposed surface loading; in particular, heavy traffic, construction equipment, and farming machinery. Potential collapse of buried pipelines poses a major risk to both the public and the environment.

Extensive research has been carried out over the last several years to study the behaviour of pipelines under different types of loading including bending, tension, and internal pressure (Ozkan and Mohareb 2009). A number of investigations have been conducted on different forms of pipeline damages such as wrinkling, denting, and fracture under operational loads (Das, Cheng and Murray 2007). Behaviour of corroded in-service pipelines has also been investigated (Dewanbabee 2009). The buckling behaviour of cylindrical shells under pure bending and external pressure has been numerically investigated (Ghazijahani and Showkati 2013). This investigation does not account for soil-pipe interaction effects. Finite element investigations on buried concrete pipes subjected to surface live loading indicate that soil-pipe interaction is necessary to study pipelines at shallow depths of bury (Noor and Dhar 2003). Various studies have been performed on pipelines in operation subjected to both static and moving surface live loading (Kabir 2006, Neya, et al. 2017). These studies showed that pipe stresses are highly dependent on both soil-pipe relative stiffness and depth of pipe bury, with maximum stresses at the pipe crown. However, the presence of internal pressure used reduces the net pressure differential. Full-scale experimental testing has been conducted on flexible empty pipes subjected to live loads (Arockiasamy, Chaallal and Limpeteeprakarn 2006). The tests were limited to intact pipe sections. In spite of the many studies reported in the literature, there exist very limited available studies on the behaviour and degradation of the structural integrity of decommissioned steel pipelines left in place underground.

2 PROBLEM FORMULATION

The initial step in determining the long-term structural integrity of decommissioned pipelines is assessing and understanding the static response of the pipeline immediately after decommissioning. The static response of a pipeline subjected to surface live load is dependent on a variety of factors including load geometry and location, soil stiffness, pipe section properties, soil-structure interaction and depth of bury. Load is transferred from the soil to the pipe section through a process known as soil arching. Soil arching describes the state where an unstable soil mass (due to translation or yield) transfers stress to an adjacent rigid body (Terzaghi 1943). In a soil block, this rigid body may be adjacent stable soil or an adjacent rigid pipeline.

As the depth of bury is reduced, the path from the surface load to the stiff pipe section becomes shorter and more direct. Since the pipe section is much stiffer than the surrounding soil, the load attracted by the pipe section is expected to increase. Based on this fundamental observation the initial analysis consists of investigating the effects of depth of soil cover on the resulting stresses and deformations of the pipe section. A reasonable critical depth is then selected to investigate the effects of wall thickness (Figure 1). Investigating variable wall thickness serves two-fold in determining the initial response of variable section thickness that may be used and investigating the long-term effects of global corrosion. Global corrosion involves the uniform wall thinning of a pipe section. Within both analyses conducted, four separate pipe sections are used, enabling the effect of pipe diameter to be observed simultaneously. Pipe diameters 20”, 24”, 28”, and 34” were used for both analyses.

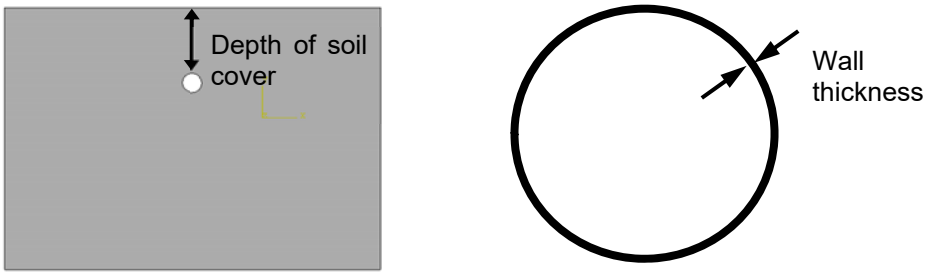

Figure 1: Analyses to be considered: effects of depth of bury (left) and wall thickness (right)

3 THE FINITE ELEMENT MODEL

All models developed for the subsequent studies were analyzed using the commercial finite element software ABAQUS. ABAQUS is commonly used throughout the industry for finite element analysis of buried pipelines subjected to a variety of loadings including surface loading, soil movement, and internal pressure, among others (Kabir 2006; Dewanbabee 2009). Results from these previously conducted analyses have been validated and corroborated with their respective experimental data.

3.1 General Model and Mesh Properties

3.1.1 Element Selection

The pipe section was modelled using the general purpose, four-node, first-order S4 shell elements with six degrees of freedom per node. These elements are recommended for thin-shell applications and have an inherent assumed large-strain formulation, allowing for use involving in-plane bending applications (Sadowski 2013). Thin-shelled structures are defined in ABAQUS as having a thickness ratio greater than 1/15 compared to a characteristic length (Dassault Systemes 2014). The characteristic length of interest is considered the pipe radius. For the 20” pipe section, a standard 3/8” wall thickness equates to a thickness ratio of 26.7; much higher than the limiting value.

The soil block was modelled using second order, ten-node, tetrahedron C3D10 solid continuum elements. The main influencing factor for the soil elements was the ability to obtain a high-quality mesh. Due to the transition from rectangular geometry of the loading and soil block to the circular geometry of the pipe section, tetrahedron elements proved most advantageous. Tetrahedral elements allow for ease of meshing around circular boundaries and are less sensitive to initial element distortion.

3.1.2 Boundary Conditions and Model Size

The boundary conditions and model size were selected such that the model is representative of a pipeline buried within an infinite soil medium. The four side surfaces were modelled with roller boundary supports, preventing translation normal to the surface while allowing for vertical displacement. The base of the block was hinged supported, preventing translation in all orthogonal directions. The boundary conditions are applied to the surface of the model, as opposed to individual nodes, implicitly restricting rotations.

The model geometric size was then optimized to reduce the influence due to the proximity of the boundary conditions. A preliminary 5 m cubic soil block was modelled. The length, width and height of the soil block were then individually increased and the resulting stresses were plotted. Optimal model size was determined as the point at which the maximum stresses converged. Based on the convergence analysis, the optimal model size was selected as L x W x H equal to 20 m x 16 m x 12 m (Figure 2).

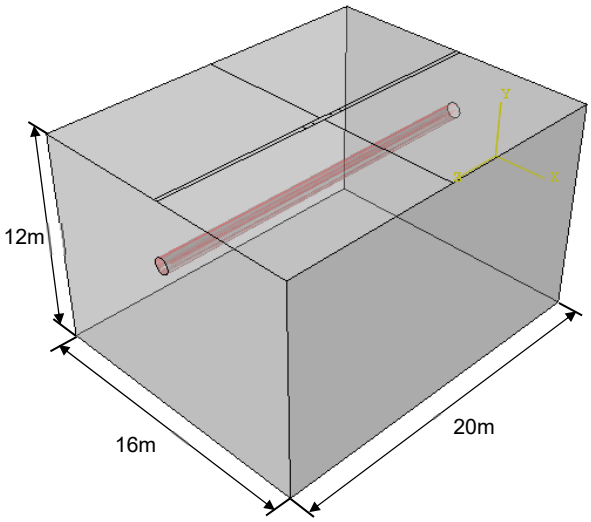

Figure 2: General model layout and geometry

3.1.3 Mesh Refinement

A mesh refinement study was performed separately for both the pipe section and the soil block. To refine the mesh of the pipe, a 34" pipe beam section was analysed. The pipe was modelled with fixed-fixed end conditions and subjected to a uniformly distributed load. The resulting stresses were compared to theoretical values obtained using Timoshenko beam theory. The number of elements around the circumference of the pipe section was increased until convergence was achieved. The aspect ratio of the elements was maintained at 1:1. Convergence occurred at approximately 30 elements around the pipe circumference.

The soil block was meshed using a biased mesh, allowing for increased mesh refinement around the pipe section and points of load application. Since the influence due to boundary conditions is negligible, the boundaries of the block can afford a more coarse mesh. A biased mesh greatly reduces the number of elements used and computational time required (Figure 3). The degree of bias was then increased, increasing the number and reducing the size of the elements at the critical locations. Convergence of the stresses occurs at approximately 100,000 elements. The same mesh size (number of elements around the pipe section and the degree of bias) was used for all subsequently smaller pipe diameter models.

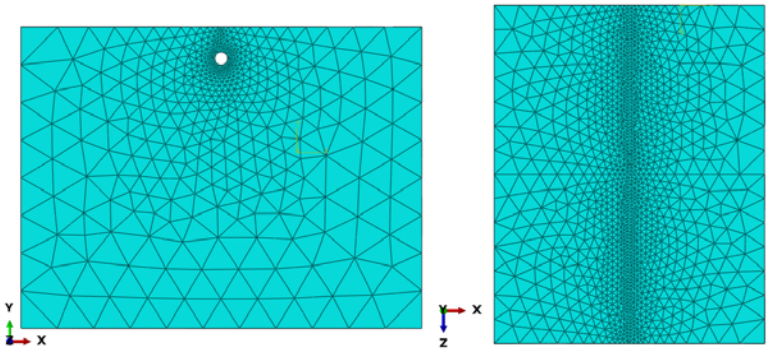

Figure 3: Finite element mesh

3.2 Material Properties

3.2.1 Pipe Section

Pipelines can be composed of various materials depending on the contents to be transported, soil conditions and stress requirements. For the purposes of this investigation, the pipeline material was chosen to be API 5L X52 steel. This steel specification is commonly used for transporting water, oil, gas, and chemicals throughout the petroleum industry. The pipeline steel was modelled as a homogenous elastic-plastic material with a yield stress, σ_y, of 415 MPa, modulus of elasticity, E, of 200,000 MPa, and Poisson's ratio, ν, of 0.3 (PM International Suppliers 2017). Material plasticity beyond the yield stress was modelled assuming a Ramberg-Osgood material relation between stress, σ, and strain, ε given by:

$$[1] \qquad \varepsilon = \frac{\sigma}{E} + \alpha\left(\frac{\sigma}{\sigma_y}\right)^n$$

where the parameter α represents the yield offset strain, assumed to be 0.2% for ductile steel; and n was modified such that the resulting stress strain curve fits with literature curves (Trifonov 2015). The nominal stresses and strains were then converted to true stress and strain to be used in ABAQUS.

3.2.2 Soil

The maximum depth of bury used in the analysis is 3.0 m of soil cover. At this depth, it is reasonable to assume the overburden consists of a single homogenous soil layer. The soil material was modelled using an elastic-perfectly plastic Mohr-Coulomb plasticity model. The Mohr-Coulomb model is recommended for use in geotechnical engineering applications to study material response under monotonic loading (Dassault Systemes 2014). The soil material was assumed to be soft clay. Soft clay is present in abundance in North America and serves as a critical soil material with its low elastic modulus and friction angle compared to other soils. Mohr-Coulomb parameters used are summarized in Table 1 (Lee 2010; Subramanian 2010):

Table 1: Soil Material Properties

Parameter	Value Used in Analysis
Mass Density, γ (kg/m^3)	18
Young's Modulus, E (MPa)	25
Poisson's Ratio, ν	0.3
Friction Angle, φ (°)	25
Dilation Angle, ψ (°)	2
Cohesive Strength, c (kPa)	100

3.3 Contact Definition

Frictional soil-pipe interaction was modelled in ABAQUS using a surface-to-surface contact definition and employing the penalty enforcement method. Penalty enforcement allows for various contact slip formulations including friction, shear stress and elastic slip. Slip between the soil and pipe surface was defined using a coefficient of static friction. The coefficient of friction, μ, was determined based on the ASCE ALA Guidelines for Design of Buried Steel Pipe (American Lifelines Alliance 2001).

$$[2] \qquad \mu = \tan\left(f\,\varphi\right)$$

The coating dependent factor, f, is attributed to the surface condition of the pipe section. A factor of 0.8 was used to represent a rough surface due to corrosion. Therefore, the coefficient of friction used was 0.36. Frictional contact was applied in the longitudinal and circumferential directions of the pipe section, while

'hard' contact was applied in the normal direction. Hard contact ensures zero penetration of the two surfaces while allowing for separation as the system deforms.

3.4 Loading

The pipeline is subjected to two load cases; dead loading including pipe self-weight and the soil overburden, and surface live load. Surface loading was taken from the Canadian Highway Bridge Design Code S6-14, utilizing the appropriate dynamic load increase factor of 1.4 for single axle loading conditions (Canadian Standards Association 2014). The maximum wheel load of a CL-800 truck is 112 kN. This load was applied over a contact area of 600 mm x 250 mm and combined with the dynamic load factor, resulting in a live load pressure of 1.045 MPa. This pressure was applied at two wheel load locations, representing a truck travelling perpendicular to the pipe axis (Figures 4 and 5).

A static non-linear finite element analysis was performed to obtain the resulting stresses and deformations. It is recognized that the system has the potential to experience large local deformations as the depth of bury and wall thickness are reduced. Therefore, non-linear geometric analysis is required.

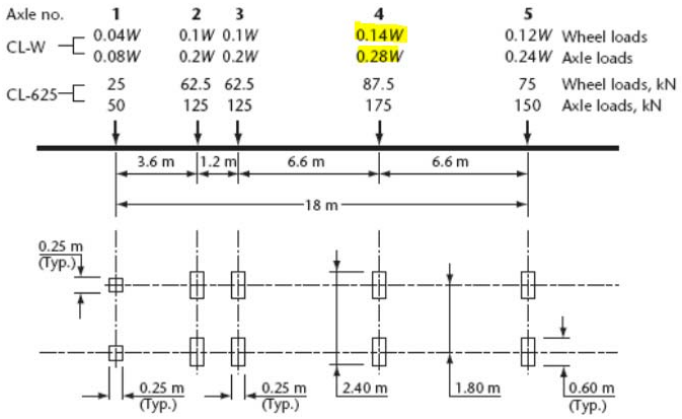

Figure 4: S6-14 CL-W loading diagram

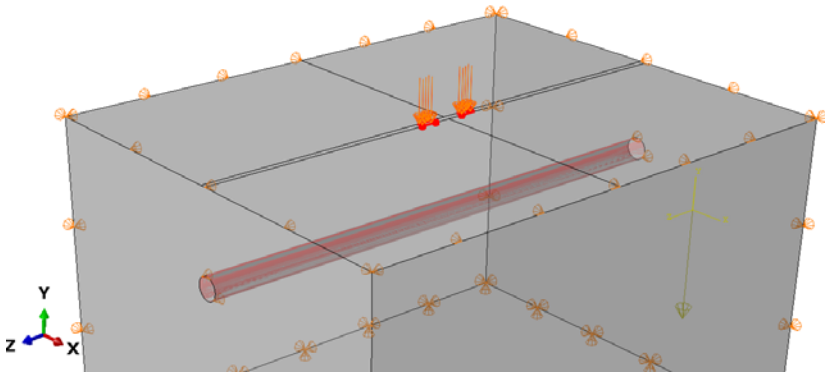

Figure 5: Load application on finite element model

4 RESULTS AND DISCUSSION

The primary results of interest include the pipe section ovalization and the resulting normal stresses: longitudinal stresses along the pipe axis arising from longitudinal bending, and circumferential hoop stresses arising from the external pressure differential and transverse soil friction. Results extracted are located directly beneath the point of one wheel load application. Stresses were obtained at the extreme fibre at the pipe crown, invert, and springline (i.e., the top-most, the bottom-most, and the mid-height points

of the pipe cross-section, respectively). The maximum stress for all pipe sections analyzed is found at the pipe crown. For the sake of brevity, only stresses at the pipe crown are plotted and discussed below. Pipe section ovalization is defined as the difference between the vertical displacements at the pipe crown and the invert.

4.1 Effect of Depth of Bury

The depth of bury is varied between 3.0 m and 0.5 m in 0.5 m increments. Wall thickness is maintained at the standard 3/8" for all diameters. As can be seen in Figure 6, both the longitudinal and hoop stresses increase in magnitude with the decrease in depth of bury. The increase in stresses is not linear, but rather exponential, indicating that the depth of bury is a significant factor affecting the resulting stress state.

As the depth of bury decreases, the live load path to the pipe becomes shorter and more direct. As such, the pipe attracts more load and the resulting stresses increase. The maximum stress is compressive and is located at the pipe crown. The compressive stresses are due to both global and local bending of the section. At depths of bury shallower than 1.0 m, the resulting stresses begin to increase rapidly and become more localized under the wheel loads (Figure 7). However, it is noted that the maximum stresses remain below the pipe yield stress.

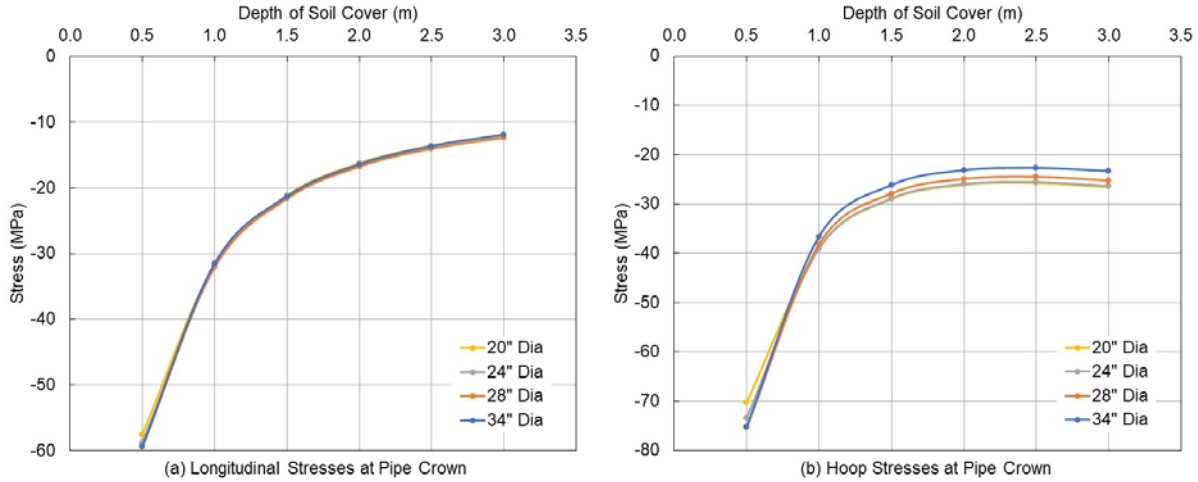

Figure 6: Effect of depth of bury – stresses at pipe crown

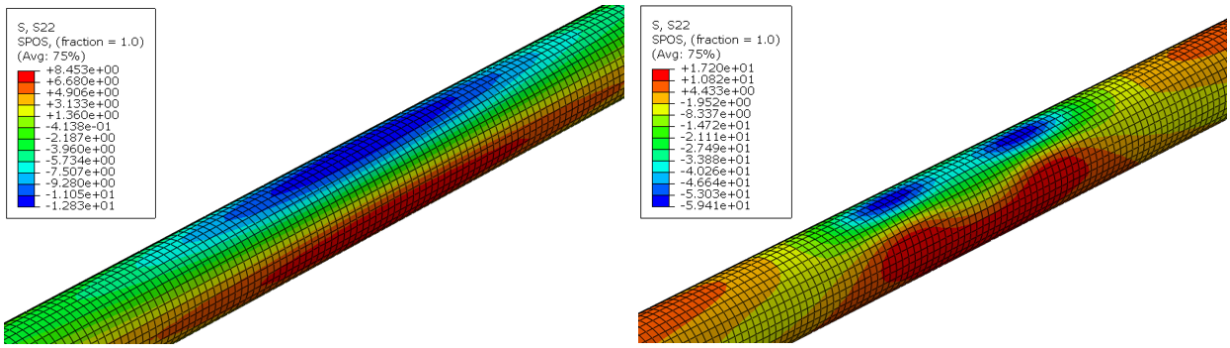

Figure 7: Depth of bury – 34" dia. pipe: Longitudinal stresses for 3.0 m (left) and 0.5 m (right)

Further, pipes of smaller diameters experience larger stresses at deeper depths of bury. As the pipe diameter is reduced, the moment of inertia of the pipe section also reduces, increasing the global bending stresses. However, as the depth of bury continues to decrease, smaller pipe diameters experience lower stresses. At shallow depths of bury, the surface load acts similar to a concentrated force applied directly to the pipe section. As a result, local bending stresses begin to govern the stress state. By maintaining a

constant wall thickness for all pipe diameters, smaller pipe diameters have a larger local wall stiffness. The increases in stresses due to reduction in pipe diameter are offset by the simultaneous reduction in diameter-to-thickness ratio. This observation is further confirmed in the wall thickness study presented in Section 4.2.

Figure 8 illustrates the effect of depth of burry on the pipe ovalization. As the depth of bury decreases, vertical ovalization also increases. As the pipe diameter decreases, smaller pipes experience smaller ovalization while the increasing trend is near identical. Smaller pipe sections have inherently smaller absolute dimensions and an increased local wall stiffness, resulting in smaller ovalization.

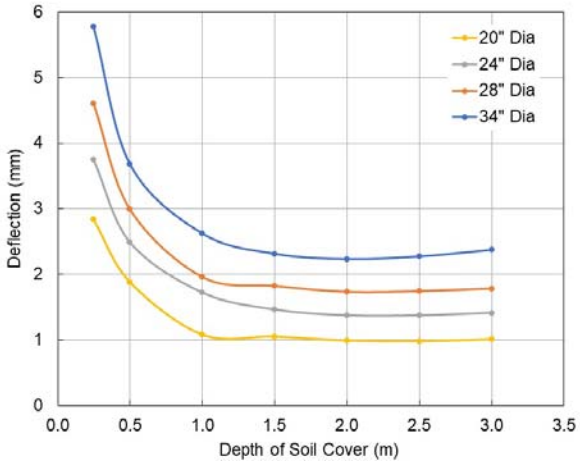

Figure 8: Effect of depth of bury on vertical ovalization

4.2 Effect of Wall Thickness

Based on the depth of bury analysis, stresses begin to become significant at approximately 1.0 m of soil cover. Therefore, the effect of wall thickness is investigated using 1.0 m soil cover. The wall thickness is varied between 5/8” (schedule 30 pipe section) and 1/16” at the extreme ends. Typical pipe sections have a common minimum thickness of 1/4", indicating that thinner thicknesses are a direct result of uniform global corrosion.

Figure 9 shows that, as the wall thickness is reduced, both the longitudinal and hoop stresses increase. However, the hoop stresses increase to a maximum value and then begin to decrease, while the longitudinal stresses continue to increase in magnitude. The increase in longitudinal stresses is due to the reduction in the section’s moment of inertia, increasing in global and local bending stresses. The reduction in the hoop stresses is due to both the localized effects of the load and the reduction in the section’s overall stiffness.

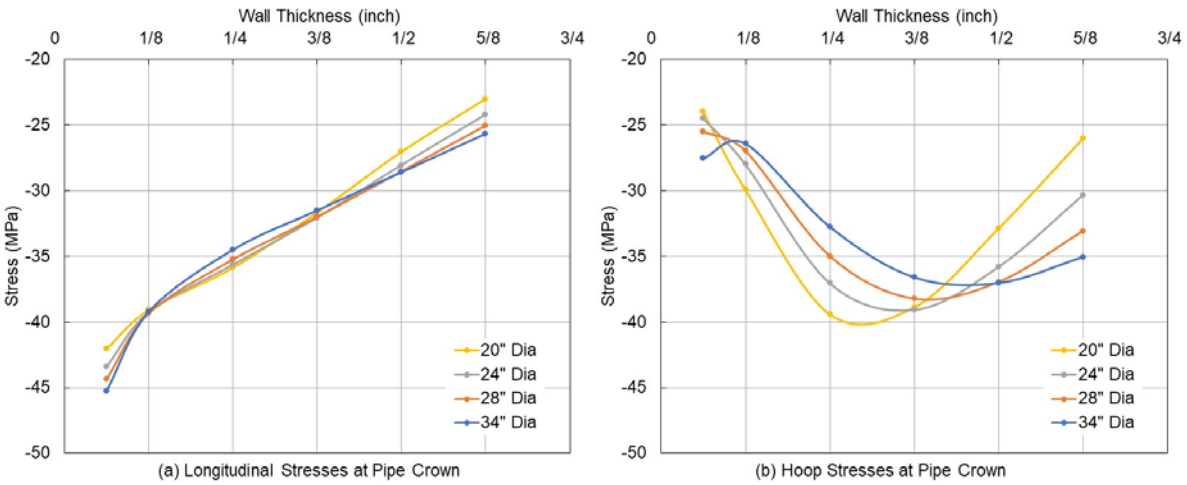

Figure 9: Effect of wall thickness on stresses at pipe crown

As the wall thickness is reduced, the load effects become more localized at the location of the wheel load. With a thick pipe wall, the stiffness of the pipe is great enough that the surface loads interact with each other. As the stiffness of the pipe reduces, the local deformations of the section increase and the surface loads act independently of one another (Figure 10). Further, the stiffness of the pipe section also reduces relative to the surrounding soil as the wall thickness is reduced. Due to the soil arching effects, as the relative stiffness of the pipe reduces, the pipe attracts less load and the soil attracts more load. This phenomenon is visualized by plotting the contact pressure for the 34” diameter pipe section. As can be seen in Figure 11, the normal contact pressure acting on the pipe section reduces as the wall thickness is reduced, indicating that the pipe is attracting less load. As the soil attracts greater portion of the load, the amount of soil slippage increases, reducing the resulting hoop stresses.

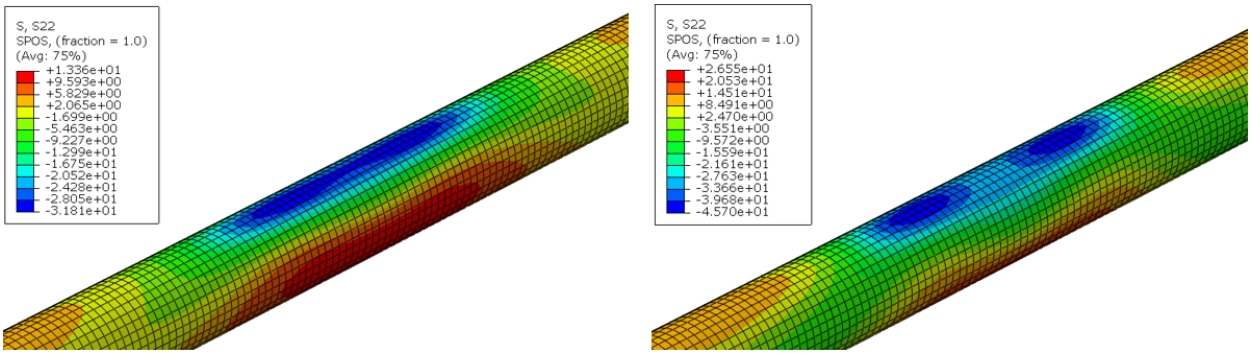

Figure 10: Effect of wall thickness – 34” dia. pipe: Longitudinal stresses for 3/8” (left) and 1/16” (right)

Figure 12 shows the variation of the resulting stresses with diameter-to-thickness, D/t, ratio. As can be seen, the resulting stresses begin to increase rapidly as the D/t ratio decreases below 100. The D/t ratio is approximately 90 for the standard 34” pipe section and 53 for the 20” pipe section. As a result, the initial conclusions of increased local stiffness offsetting the increase in stresses of smaller pipe diameters during the depth of bury analysis are confirmed.

Lastly, examining the effects of wall thickness on pipe ovalization, Figure 13 shows that the degree of pipe ovalization increases with the wall thickness decreases. The increase is nearly linear, due to the reduction in pipe section stiffness. The increase begins to plateau at very thin wall thicknesses due to increased soil slippage and reduction in the load attracted by the pipe section.

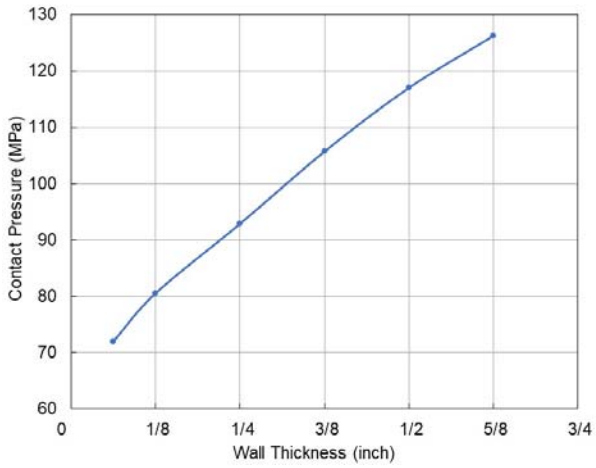

Figure 11: Effect of wall thickness on the contact pressure acting on 34” pipe section

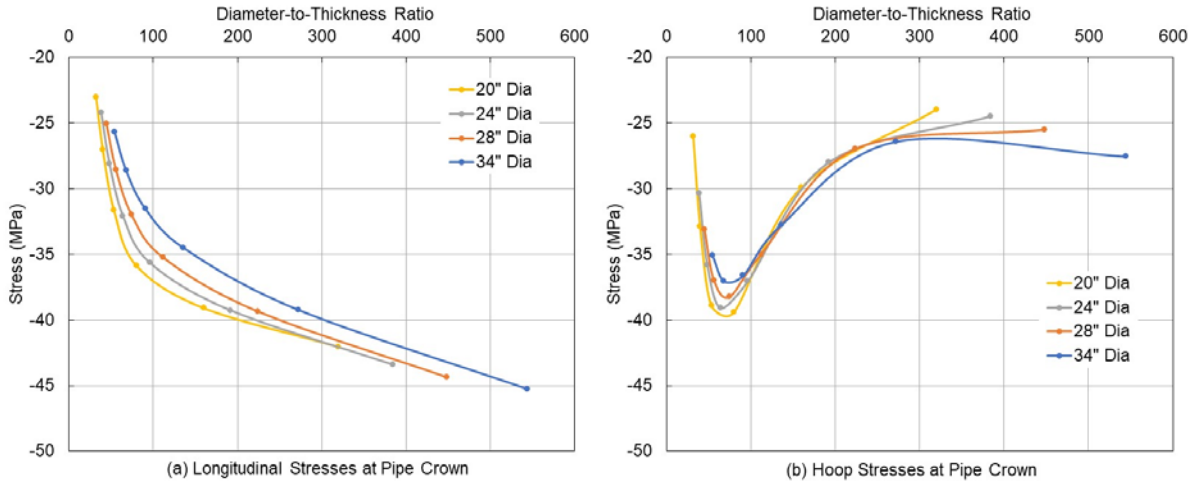

Figure 12: Effect of diameter-to-thickness ratio on the stresses at pipe crown

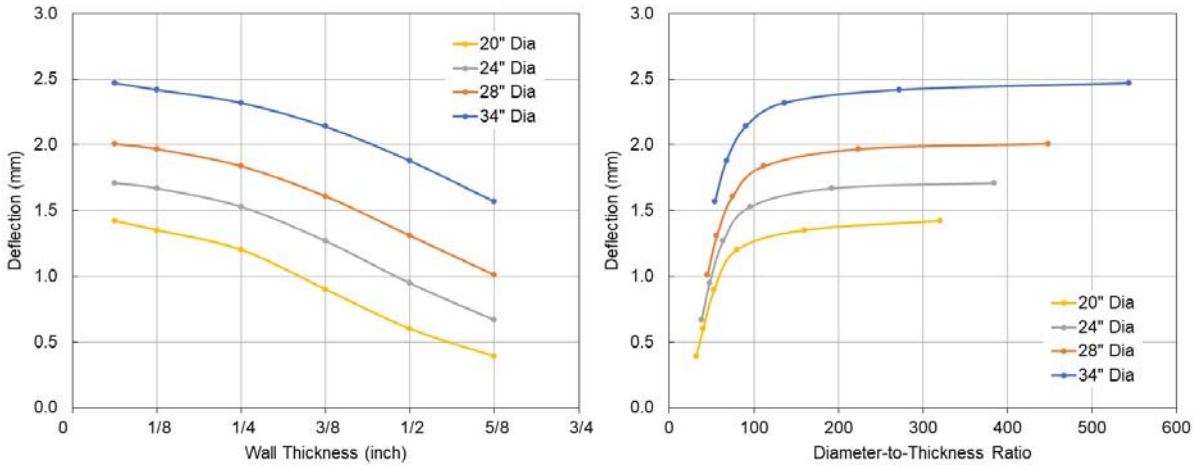

Figure 13: Vertical ovalization: Effect of wall thickness (left) and diameter-to-thickness ratio (right)

5 CONCLUSIONS

Finite element analysis of in-*situ* decommissioned pipelines subjected to surface live load was investigated. The effects of depth of bury, pipe diameter, and wall thickness on the resulting stress state were obtained and discussed. The following primary conclusions were drawn:

1. As the depth of bury decreases, the resulting longitudinal and hoop stresses both increase. The increase is exponential indicating depth of bury is a significant factor influencing the load path and the resulting stress state.

2. The stresses become increasingly significant at depths of soil cover less than 1.0 m. At depths of bury greater than 1.0 m, the stresses converge at a much lower stress value.

3. As the wall thickness is reduced, the resulting longitudinal and hoop stresses begin to increase. The longitudinal stresses increase due to a reduced moment of inertia and increased bending stresses. The hoop stresses initially increase and then begin to decrease as the load becomes more localized, the pipe attracts less load, and the degree of soil slippage increases.

4. As the pipe diameter decreases, the resulting stresses typically increase. However, this increase is offset by a simultaneous reduction in the D/t ratio if the wall thickness is kept constant.

5. Pipe ovalization increases with the decrease in the depth of bury and the wall thickness~~es~~ for all pipe diameters.

Despite the increase in stresses with reduction of the depth of bury, pipe diameter, and wall thickness, the resulting stresses remain well below the pipe yield stress. It is observed that at reasonably deep soil cover and standard wall thicknesses, decommissioned pipelines pose little risk of collapse due to typical surface live load applied immediately after decommissioning.

The location and direction of maximum stresses change as the wall thickness of the pipe section changes. This is of significant importance when examining the effects of local corrosion. The criticality of local corrosion geometry and location is highly dependent on the location of the maximum stresses. It is necessary for the above investigations to be extended to include the effects of local corrosion in determining the structural response and capacity of buried decommissioned pipelines subjected to surface loading.

Acknowledgements

This investigation reported in the paper is financially supported by a research contract from Enbridge Pipeline Inc. The valuable input and feedback provided by Dr. Robert Satchwell (Manager Engineering, MP CAN Execution) and Mr. Ryan Champney (Manager, Pipeline Design, MP CAN) of Enbridge are gratefully acknowledged.

References

American Lifelines Alliance. 2001. "Appendix B: Soil Spring Representation." In *Guidelines for the Design of Buried Steel Pipe*, pp. 68-69. ALA.

Arockiasamy, M., Chaallal, O., and Limpeteeprakarn, T. 2006. "Full-Scale Field Tests on Flexible Pipes under Live Load Application." *Journal of Performance of Constructed Facilities*, pp. 21-27.

Canadian Standards Association. 2014. *Canadian Highway Bridge Design Code.* 11. Mississauga, Ontario: CSA Group.

Das, S., Cheng, R.J.J., and Murray, D.W. 2007. "Prediction of the fracture life of a wrinked steel pipe subject to low cycle fatgue." *Canadian Journal of Civil Engineering* 34 (9): 1131-1139.

Dassault Systemes. 2014. "Abaqus Analysis User's Guide." April 23. Accessed Decemeber 31, 2017. http://abaqus.software.polimi.it/v6.14/books/usb/default.htm.

Dewanbabee, H. 2009. *Behaviour of Corroded X46 Steel Pipe under Internal Pressure and Axial Load.* Windsor: University of Windsor.

Ghazijahani, T.G. and Showkati, H. 2013. "Experiments on cylindrical shells under pure bending and external pressure." *Journal of Constructional Steel Research*, 109-122.

Kabir, A. 2006. *Soil-Structure Interaction Analyses of Buried Rigid Pipes under Surface Loads.* Dhaka: Bangladesh University of Engineering & Technology.

Lee, H. 2010. *Finite element analysis of a buried pipeline.* Manchester: University of Manchester.

Nazemi, N. and Das, S. 2010. "Beahviour of X60 Line Pipe Subjected to Axial and Lateral Deformations." *Journal of Pressure Vessel Technology* 132 (3): 7.

Neya, B., Ardeshir, M., Delavar, A., and Bakhsh, M. 2017. "Three-Dimensional Analysis of Buried Pipes Under Moving Loads." *Open Journal of Geology* 7: 1-11.

Noor, M. and Dhar, A. 2003. "Three-Dimensional Response of Buried Pipe under Vehicle Loads." *ASCE International Conference on Pipeline Engineering and Construction.* Baltimore: ASCE. 658-665

Ozkan, I.F. and Mohareb, M. 2009. "Testing and Analysis of Steel Pipes under Bending, Tension, and Internal Pressure." *Journal of Structural Engineering* 132 (2): 187-189.

PM International Suppliers. 2017. *API 5L X Grades.* http://www.api5lx.com/api5lx-grades/.

Sadowski, A. 2013. "Solid or shell finite elements to model thick cylindrical tubes and shells under global bending." *Internation Journal of Mechanical Sciences* 74: 143-153.

Subramanian, N. 2010. "Appendix C - Properties of Soils." In *Design of Steel Structures*, 1396-1400. Oxford: Oxford University Press.

Terzaghi, K. 1943. "Arching in Ideal Soils." Chap. 5 in *Theoretical Soil Mechanics*, 66-76. New York: John Wiley & Sons.

Trifonov, O. 2015. "Numerical stress-strain analysis of buried steel pipelines crossing active strike-slip faults with an emphasis on fault modeling aspects." *Journal of Pipeline Systems Engineering and Practice* 6 (1).